Spectrum of Engineering Sciences
ISSN (e) 3007-3138 (p) 3007-312X Volume 3, Issue 10, 2025

# STRUCTURAL, MAGNETIC AND MAGNETO TRANSPORT PROPERTIES OF FESNTI HALF HEUSLER ALLOYS THIN FILM SYNTHESIZED BY ELECTRODEPOSITION METHOD

**Arooj Fatima[1], Nizam Ahmad[*2], Sidra Dildar[3], Muhammad Sajjad[4], Ghazal Sharmeen[5], Maryum Iram [6], Sadia Manzoor[7]**

[1,*2]*Centre of Excellence in Solid State Physics, University of the Punjab, Lahore, Pakistan*
[3,6,7]*Institute of Physics, Bahauddin Zakaria University Multan*
[4]*Department of Physics, University of Education, Lahore*

[1]barbooj16@gmail.com, [*2]nizamah17@gmail.com, [3]sidradildar786@gmail.com, [4]muhammadsajjad8947@gmail.com, [5]ghazal.sharmeen@yahoo.com, [6]maryumiram7@gmail.com, [7]sadiamanzoor230598@gmail.com

DOI:https://doi.org/10.5281/zenodo.17277654

**Keywords**
*FeSnTi Half Heusler Alloys, Structural, Magnetic, Magneto Transport Properties, Thin Film, Synthesized, Electrodeposition Method, X-ray diffraction*

**Article History**
*Received: 12 August 2025*
*Accepted: 22 September 2025*
*Published: 06 October 2025*

**Copyright** @Author

**Corresponding Author: ***
**Nizam Ahmad**

**Abstract**

*Heusler alloys are ferromagnetic in nature but the tow of the ingredients of this alloy are itself not the magnetic. Heusler Alloy has been prodigious investigations from its recognition and discovery. FeSnTi based half Heusler alloy thin films are prepared by utilizing electrodeposition technique with varying applied voltage from 0.6 V to 1.0 V with an interval of 0.1 V. The electrodeposited FeSnTi thin films are characterized by XRD and VSM. XRD studies reveal mixed phases for the samples deposited at applied voltage of 0.6 V and 0.7 V. At 0.8 V of applied voltage, a chemical shift from mixed phases to pure cubic FeSnTi phase of half Heusler alloy thin film is observed. With further increase in applied voltage i.e. 1.0 V, only strengthening and phase stability of pure cubic FeSnTi phase of half Heuslar alloy thin film is observed. The ferromagnetic behavior is observed for all the samples. The highest value of saturation magnetization 'Ms' and coercivity 'Hc' i.e. '49.0 emu/cm$^3$' and '925.9 Oe' of FeSnTi Heusler alloy thin film is observed at 1.0 V of applied voltage due to the formation of pure cubic FeSnTi stable and strengthened phase. Magnetocrystalline anisotropy ($K_{eff}$) is calculated to be 9.77E+9 erg/cm$^3$. Magneto transport properties are investigated for the optimized sample of Heuslar alloy thin films.*

## INTRODUCTION

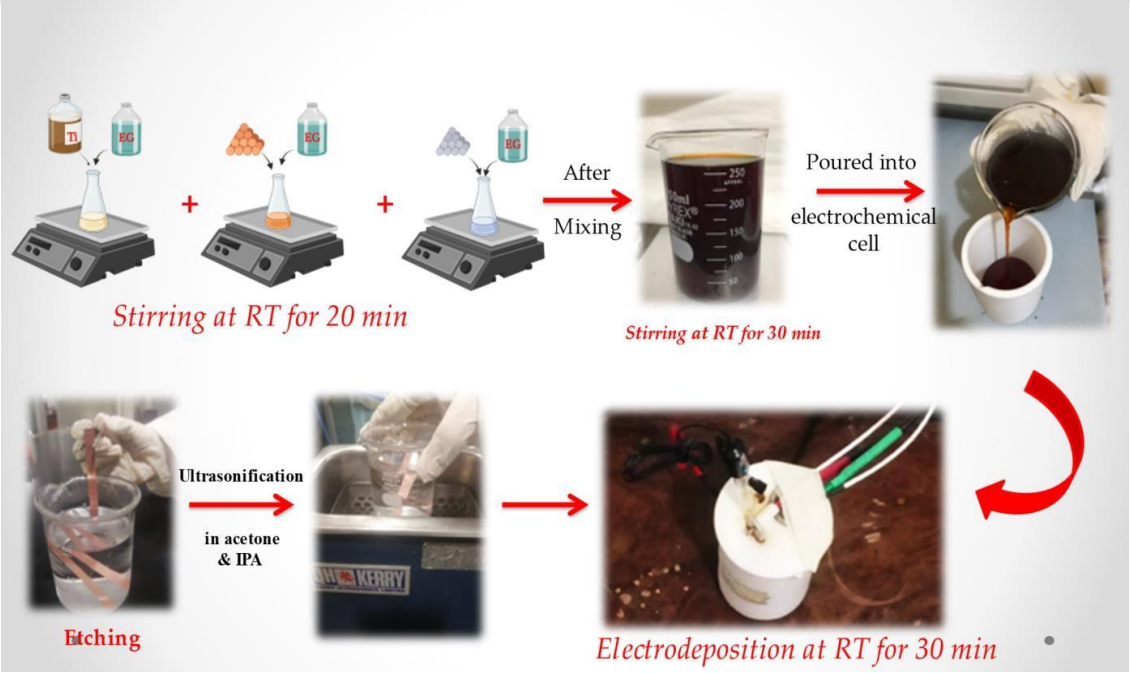
Due of their potential impacts on spintronics, half-metallic ferromagnets (HMFs) have garnered a great deal of interest recently [1-3]. Due to the presence of a semiconductor-like gap in one spin band around the Fermi level and a metallic-like spin band in another, the HMFs exhibit significant spin-polarization of the conduction electrons at this level. HMFs are very intriguing from a theoretical and technical perspectives since many magnetoelectronic devices relied on an asymmetry in the ratio of

majority- and minority-spin carriers [3–4]. The fully (100%) spin- polarized current of HMFs can be employed as a spin injector in a wide variety of spin-dependent devices. Numerous substances, in particular Heusler compounds [5–10], diluted magnetic semiconductors [11–12], zinc-blende pnictides and chalocogenides of transition metal compounds [13–27], metal oxides [18–20], have been discovered to exhibit the half-metal properties. The X2YZ type of intermetallic ternary Heusler alloys is where X and Y are transition metals and Z is an element from the main group [21]. Researching and synthesizing novel materials can be an imperative step when taking into consideration the applications of half-metallic Heusler alloys in spintronic device applications. The Heusler alloys in this context relate to the huge family of Fe- based compounds. Fe2CrSi were synthesized experimentally in 2007 and were projected to be half-metallic [22]. Then, this alloy has undergone various study operations [23–24]. Investigations on the half-metallicity of Fe-based Heusler alloys are currently insufficient when comparable to Co- or Mn-based alloys. Many more Fe-based Heusler alloys' electrical structures are not yet identified. In this publication, we evaluated the structure and magnetic characteristics of FeSnTi Heusler alloys.

**Experimental method**

The iron tin titanium electrolytes were prepared by mixing 0.05M of iron tetra chloride ($FeCl_2.4H_2O$), 0.05M of titanium tetra butaoxide ($C_{16}H_{36}O_4Ti$) and 0.05M of tin chloride dehydrate ($SnCl_2.2H_2O$) in ethylene glycol (EG) separately. The stirring was done at room temperature of these electrolyte, separately. After that three electrolytes were mixed together and then stirred at room temperature for 30 min. The Ph of the electrolyte was 2. In the final electrolyte boric acid was added as a buffering agent and sodium chloride was added to increased the conductivity and ascorbic acid was added as a complexing agent. The measured pH of the electrolyte was remain acidic i.e. Ph 2. After that the FeSnTi electrolyte poured into chemical cell. In the electrochemical cell copper electrode was used as a counter electrode. Firstly copper substrate was etched with the diluted HCl and then ultrasonification of copper substrate was done in acetone and then in isopropyl alcohol for 15 min, seperately in order to remove further residual impurities. The electrodeposition was done for 30 min by varying the applied potential from 0.6 V to 1V with the help of VERSA stat 4.

| Sample | Chemical Equation | Weight |
|---|---|---|
| Titanium (Ti) | $C_{16}H_{36}O_4Ti$ | 2.38 ml |
| Iron (Fe) | $FeCl_2.4H_2O$ | 1.386g |
| Tin (Sn) | $SnCl_2.2H_2O$ | 1.57g |




**Results and Discussions**

Introduction

FeSnTi half-Heuslar alloy thin films were prepared by employing electrodeposition technique, with varying applied voltage from 0.6 V to 1.0 V. To evaluate the properties of these thin films, different techniques were used. Cyclic voltammetry was performed to find out about the reduction potential at working electrode. X-ray diffraction (XRD) technique was used for the structural analysis. For magnetic analysis vibrating sample magnetometer (VSM) was used. The arrott plots exhibits the convex shape that confirms the ferromagnetic nature. Keff is found by slope of straight line of magnetization vs. 1/H2 curves. Results for all the techniques are discussed below in detail.

**Cyclic voltammetry**

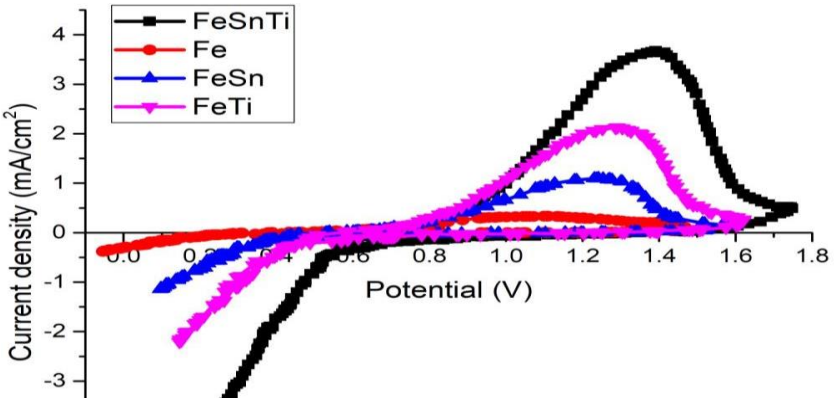



**Figure 1.1 The CV curves of FeSnTi, Fe, FeSn, and FeTi.**

The CV curves of FeSnTi were observed at a scan rate of 0.05 mv/s. Firstly, the peaks for Fe, FeSn, and maximum at point 1.4V for FeSnTi (anodic peak current ($i_{pa}$) for oxidation at the anodic peak potential ($E_{pa}$). FeTi were observed individually which shows very little value of Current. Then the current reaches peak

**Structural Analysis**

Figure 4.1 (a-b) shows the XRD patterns of electrodeposited FeSnTi Heuslar alloy thin films with

fixed deposition time of 30 minutes. Mixed phases of FeSnTi-cubic and FeSn2-tetragonal were observed at an applied voltage of 0.6 V and 0.7 V as can be seen in Fig.4.1 (a). All the planes of (200), (220), (222), (400), (331) and (103), (202), (112) & (203) matched well with the JCPD's card no. 47-1635 and exhibited cubic structure having space group F-43m. While the plane of (211) matched with the JCPD's card no. 04-0745, exhibited tetragonal structure. At 0.8 V of applied voltage, the phase shift from mixed phases to phase pure FeSnTi was observed, as shown in Fig. 4.1 (b). For all the applied voltage of FeSnTi films, the preferred orientation is along (200) plane was observed. Due to internal stresses and minimization of surface energy, crystallites preferential growth along certain plane occurs. No phase change was observed with further increase in applied voltage i.e 1.0 V. Only strengthening and stability of cubic phase of FeSnTi half-heuslar alloy electrodeposited thin films was observed.

IEER
Institute for Excellence in Education & Research

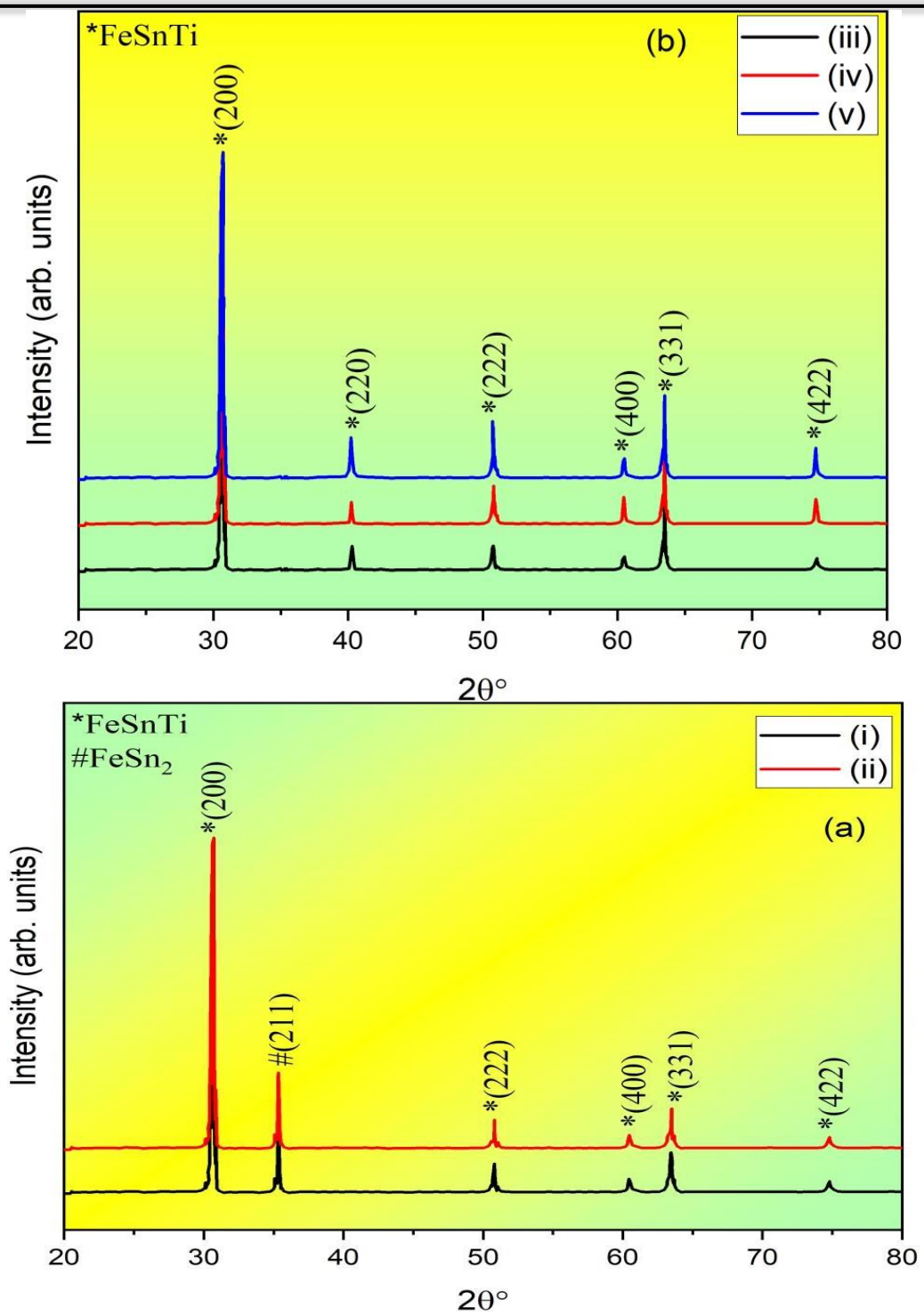



**Figure 1.2 XRD patterns of electrodeposited FeSnTi thin films with varying applied voltage from (a) 0.6 V-0.7 V & (b) 0.8 V to 1.0**

By utilizing equation (1.1) and (1.2) crystallite size and dislocation density of FeSnTi half-Heusler alloy electrodeposited thin films (B.D Cullity1978)

$$t = \frac{0.9\,\lambda}{\beta cos\theta}$$

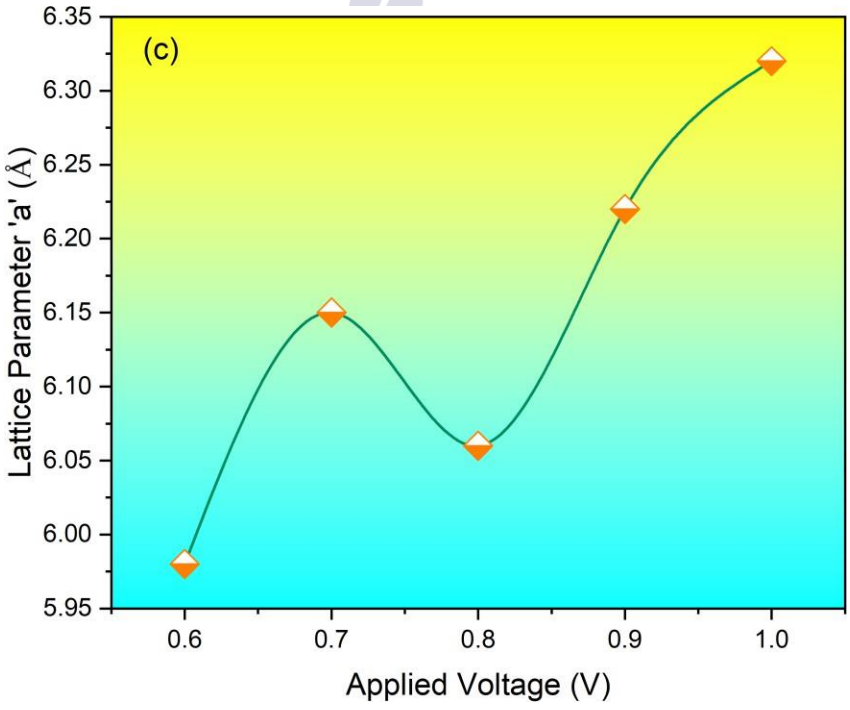
$$\delta = \frac{1}{t^2} \quad —$$

Where "$t$" is the average crystallite size, "$\lambda$" is the wavelength of Cu-$\lambda$ used in X-ray diffraction,
"$\beta$" is the full width at the half maxima (FWHM).
Lattice parameter '$a$' and unit cell volume 'V' for electrodeposited FeSnTi Heuslar alloy thin films are calculated using equation 4.3 & 4.4.

$$1/d^2(hkl) = (h^2 + k^2+l^2)/a^2 \quad (1.3)$$

$$V = a^3 \quad (1.4)$$

Figure 1.2 shows the variation of (a) crystallite size & dislocation density, (b) lattice parameter :a' and (c) Unit cell volume 'V' of FeSnTi as a function of applied voltage from 0.6 V to 1.0 V respectively. Initially, the crystallite size increases from 0.6 V to 0.7 V, having mixed phases. A decrease in crystallite size is observed at 0.8 V of applying voltage due to the chemical shift from mixed phases to pure FeSnTi cubic phase as can be seen in Fig. 4.1. At 0.9 V of applying voltage, the crystallite size increases due to the formation of pure cubic FeSnTi thin films. With further increase in voltage upto 1.0 V, increase in crystallite size was observed due to the increased strengthening and crystallinity of pure cubic FeSnTi phase.
Dislocation density shows the inverse behavior of crystallite size as shown in Fig 1.2 (b). The presence of dislocations and defects during the deposition process may be due to micro-strain present in the film. The variation of lattice parameter 'a' and unit cell volume 'V' as a a function of applied voltage from 0.6 V to 1.0 V are shown in Fig. 1.2 (c & d).



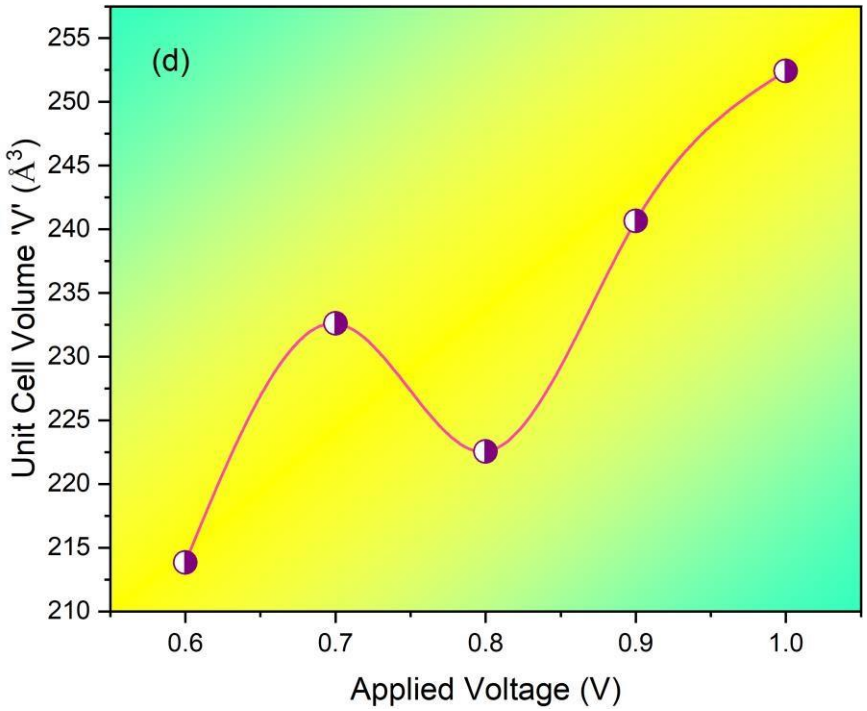



**Figure 1.3 Varition of (a) crystallite size & dislocation density, (b) Lattice parameter 'a' and (c) Unit cell volume 'V' of FeSnTi thin films as a function of applied voltage varying from 0.6 V to 1.0 V**

IEER
Institute for Excellence in Education & Research

**Magnetic Properties**

Lake Shore-7407 Vibrating sample magnetometer (VSM) was used to evaluate the magnetic properties of electrodeposited FeSnTi Heusler alloy thin films. Figure 1.3 (a-b) shows the magnetic hysteresis (M-H) loops of electrodeposited FeSnTi Heuslar alloy thin films with applied voltage varying from 0.6 V to 1.0 V, obtained at room temperature at an applied field of ±10kOe. All the samples shows the soft ferromagnetic behavior with low values of coercivity.

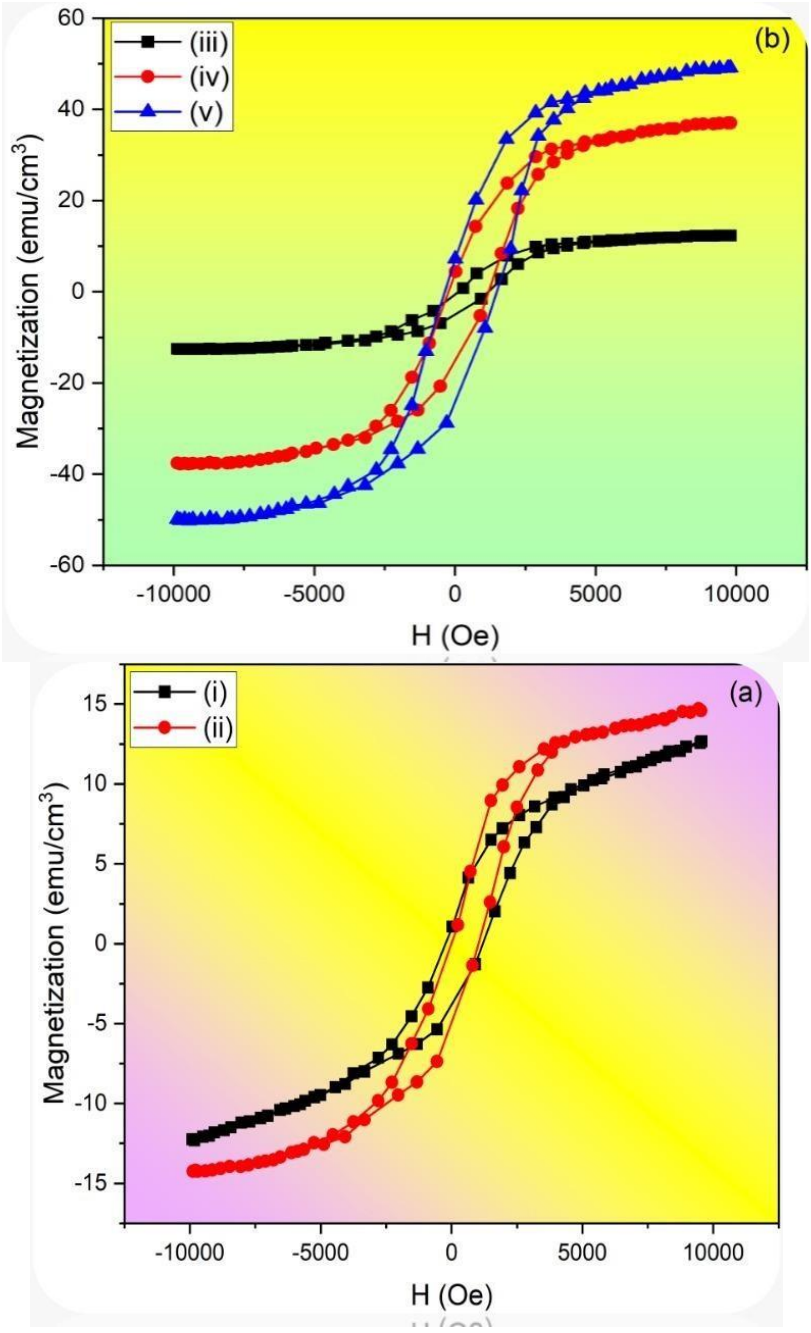



**Figure 1.4 M-H loops of electrodeposited FeSnTi Heusler alloy thin films with varying applied voltage from 0.6 V to 1.0 V**

The saturation magnetization 'Ms' and coercivity 'Hc' of FeSnTi Heusler alloy thin films as a function of applied voltage varying from 0.6 V to 1.0 V in Fig. 1.4 (a & b). The highest value of saturation magnetization 'Ms' and coercivity 'Hc' can be seen in Fig. i.e. '49.0 emu/cm$^3$" and '925.9 Oe' of FeSnTi Heusler alloy thin film was observed at 1.0 V applied voltage due to the formation of pure cubic FeSnTi stable and strengthened phase as .4

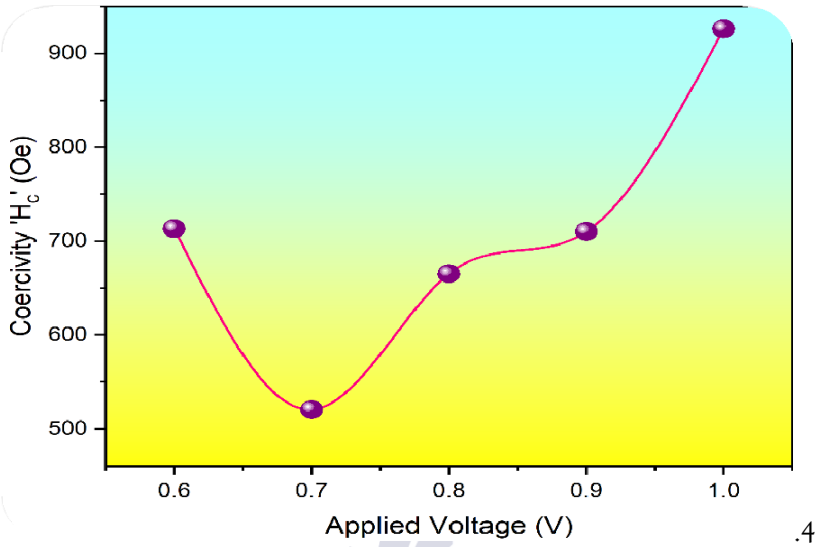



**Figure 1.5 Varition of coercivity 'Hc' of FeSnTi thin films as a function of applied voltage from 0.6 V to 1.0 V**

**Arrot Plots**

We have these graphs between square of magnetization and M/H loop to confirm the ferromagnetic nature of sample at 0.8V, 0.9V and 1V. The convex curves confirming the ferromagnetic order.

IEER
Institute for Excellence in Education & Research

0.9

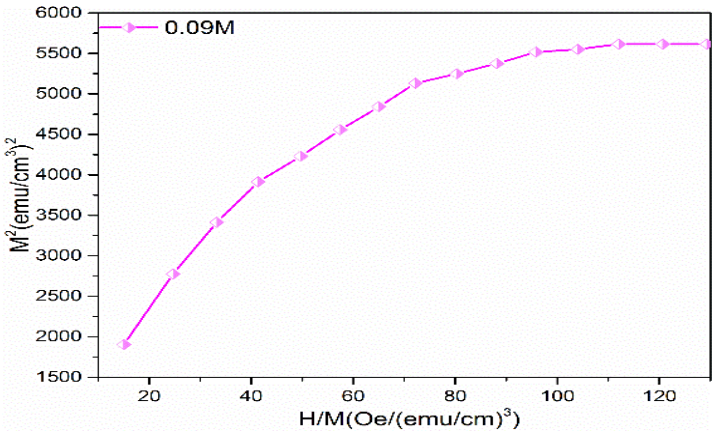



**Figure 1.6 Graphs between square of magnetization and M/H loop as a function of applied voltage from 0.6 V to 1.0 V**

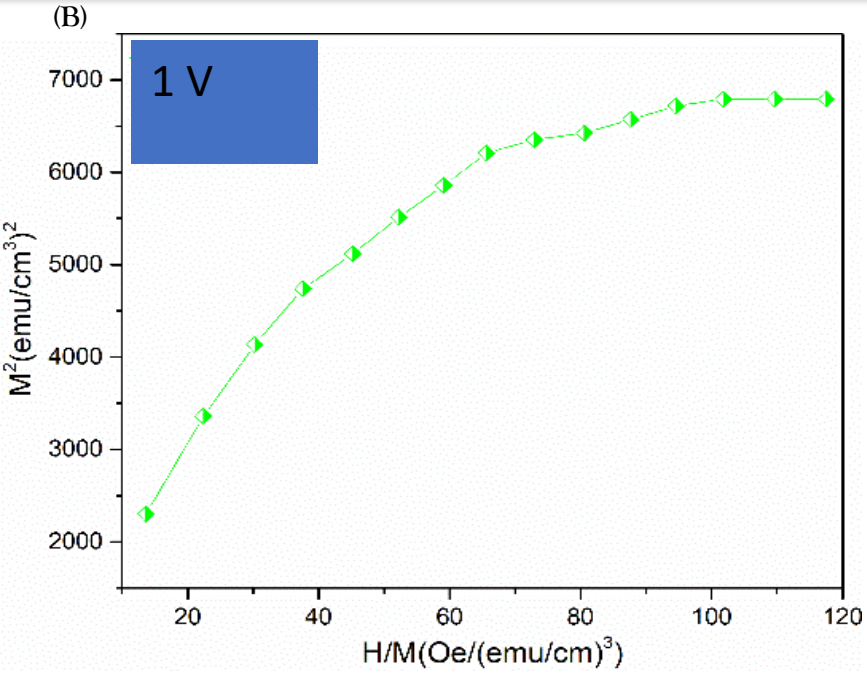
**Law of approach to Saturation**

is an important parameter which may affect the magnetic behavior of material. Usually changes in magnetization at high value of external fields is small. In this region, the magnetization and field can be related in the form of "Law of Approach to Saturation" given in these equations.

$$M = M_s\left[1 - \frac{a}{H} - \frac{b}{H^2}\right] + \chi H \quad \text{(A)}$$

$$b = \frac{2}{105}\frac{8K_{eff}}{M_s^2}$$

IER
Institute for Excellence in Education & Research




$\chi H$ represents the forced magnetization and is negligible at temperature below Curie temperature. Constant '*a*' represents the effects of micro-stress and '*b*' represents inclusion from anisotropy. Magnetocrystalline anisotropy ($K_{eff}$) is related to constant "*b*" for cubic this equation.

The following plots indicate that role of microstress can be neglected. $M_S$ values in Eq. A were obtained by straight line extrapolation of magnetization to $1/H^2 \rightarrow 0$. $K_{eff}$ is the found by slope of straight line of magnetization vs. $1/H^2$ curves in terms of Eq. B.

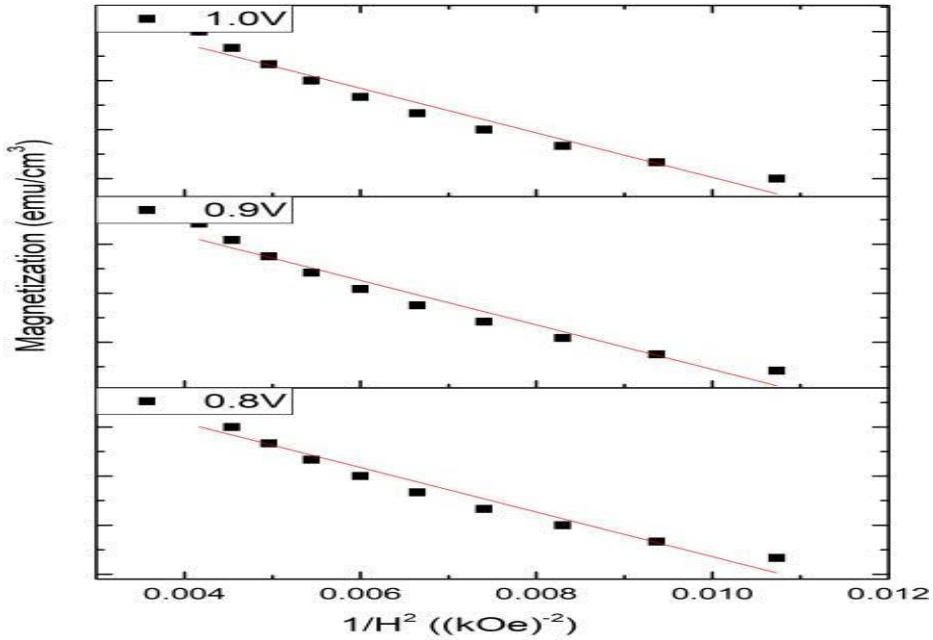



**Figure 1.7 Plots of magnetization and $1/H^2$ resulted in straight line as a function of applied voltage from 0.6 V to 1.0 V**

The Traces indicate that the micro stress role can be ignored. ms values. in Eq. A were obtained by direct extrapolation of magnetization to 1/H2→0. Keff is the slope of the magnetic
straight line with respect to the 1/H2 curves in terms of Eq. B.
Th following table give values for the optimized samples at 0.8V, 0.9V, and 1V

| Potential (V) | $K_{u1}$ (erg/cm$^3$) | Ms (emu/cm$^3$) |
|---|---|---|
| 0.8 | 7.34E+10 | 12.32 |
| 0.9 | 8.47E+10 | 36.96 |
| 1.0 | 9.77E+9 | 49.03 |

**Magneto-Transport Properties**

Negative magnetoresistance, as shown in Fig.1.8 can prevail under high current flux states which can results in interfacial diffusion thereby limiting spin injection/reorientation and eventually magnetoresistance. The anti-phasic limits also contribute basically to negative magnetoresistance.

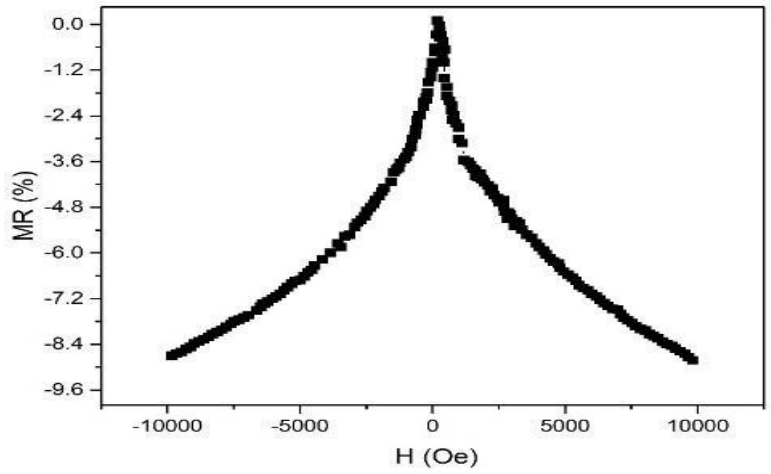



**Figure 1.8 Plot of Magnetoresistance**

**Magnetoresistance can be find out by the following formula.**

$$MR = [\frac{\rho H - \rho max}{\rho max}] x100 \quad (1.5)$$

Where $\rho_H$ is the resistance change when there is no magnetic field and $\rho_{max}$ is the resistance change when the magnetic field is present.

**Conclusions**

The constituent elements of Heuslar alloys are not necessarily magnetic, however, Heusler alloys are ferromagnetic in nature. FeSnTi based half Heusler alloy thin films were prepared by utilizing electrodeposition technique with varying applied voltage from 0.6 V to 1.0 V. Mixed crystal phases were observed for the samples prepared at low applied voltages, i.e 0.6 V and 0.7 V. A chemical shift from mixed phases to pure cubic FeSnTi phase of half Heusler alloy thin film was observed at applied voltage of 0.8 V. With further increase in applied voltage, i.e. 1.0 V, only strengthening and phase stability of pure cubic FeSnTi phase of half Heuslar alloy thin film was observed. The ferromagnetic behavior was observed for all the samples. The highest value of saturation magnetization 'Ms' and coercivity 'Hc' i.e. '49.0 emu/cm$^3$" and '925.9 Oe' of FeSnTi Heusler alloy thin film was observed at 1.0 V of applied voltage. This strengthening in magnetization capability was observed due to the formation of pure cubic FeSnTi stable and strengthened crystal phase. Magnetocrystalline anisotropy was calculated for the structurally stable thin films. Magneto crystallineanisotropy ($K_{eff}$ ) was observed to be 9.77E+9 erg/cm$^3$ . Magneto transport properties were also investigated and negative magnetoresistance was observed due to the formation of antiphase boundaries.

IEER
Institute for Excellence in Education & Research

**REFERENCES**

Julliere, M., 1975. Tunneling between ferromagnetic films. *Physics letters A*, *54*(3), pp.225-226.

Wolf, S.A., Awschalom, D.D., Buhrman, R.A., Daughton, J.M., von Molnár, V.S., Roukes, M.L., Chtchelkanova, A.Y. and Treger, D.M., 2001. Spintronics: a spin- based electronics vision for the future. science, 294(5546), pp.1488-1495.

De Groot, R.A., Mueller, F.M., Van Engen, P.G. and Buschow, K.H.J., 1983. New class of materials: half-metallic ferromagnets. Physical Review Letters, 50(25), p.2024.

Prinz, G.A., 1998. Magnetoelectronics. science, 282(5394), pp.1660-1663.

Chen, X.Q., Podloucky, R. and Rogl, P., 2006. Ab initio prediction of half-metallic properties for the ferromagnetic Heusler alloys Co 2 M Si (M= Ti, V, Cr). *Journal of applied physics*, *100*(11), p.113901.

Özdog, K., Galanakis, I., Şaşıog, E. and Aktaş, B., 2007. Defects-driven appearance of half-metallic ferrimagnetism in Co–Mn-based Heusler alloys. *Solid state communications*, *142*(9), pp.492-497.

Kandpal, H.C., Fecher, G.H. and Felser, C., 2007. Calculated electronic and magnetic properties of the half-metallic, transition metal based Heusler compounds. *Journal of Physics D: Applied Physics*, *40*(6), p.1507.

Liu, G.D., Dai, X.F., Liu, H.Y., Chen, J.L., Li, Y.X., Xiao, G. and Wu, G.H., 2008.

Mn 2 co z (z= al, ga, in, si, ge, sn, sb) compounds: Structural, electronic, and magnetic properties. *Physical Review B*, *77*(1), p.014424.

Özdog, K. and Galanakis, I., 2009. First-principles electronic and magnetic properties of the half-metallic antiferromagnet Cr2MnSb. *Journal of magnetism and magnetic materials*, *321*(15), pp.L34-L36.

Sharma, V., Solanki, A.K. and Kashyap, A., 2010. Electronic, magnetic and transport properties of Co2TiZ (Z= Si, Ge and Sn): A first-principle study. *Journal of Magnetism and Magnetic Materials*, *322*(19), pp.2922-2928.

Galanakis, I. and Mavropoulos, P., 2003. Zinc-blende compounds of transition elements with N, P, As, Sb, S, Se, and Te as half-metallic systems. *Physical Review B*, *67*(10), p.104417.

M. Asif, M. Adil Pasha, S. Shafiq, and I. Craine, *Inverge J. Soc. Sci.* **1**, 56–65 (2022). https://doi.org/10.63544/ijss.v1i1.6

Xu, Y.Q., Liu, B.G. and Pettifor, D.G., 2003. Half-metallic ferromagnetism of MnBi in zincblende phase. *Physica B: Condensed Matter*, *329*, pp.1117-1118.

Yao, K.L., Gao, G.Y., Liu, Z.L. and Zhu, L., 2005. Half-metallic ferromagnetism of zinc-blende CrS and CrP: a first-principles pseudopotential study. *Solid state communications*, *133*(5), pp.301-304.

Yao, K.L., Gao, G.Y., Liu, Z.L., Zhu, L. and Li, Y.L., 2005. Half-metallic ferromagnetic semiconductors of V-and Cr-doped CdTe studied from first- principles pseudopotential calculations. *Physica B: Condensed Matter*, *366*(1-4), pp.62-66.

Ge, X.F. and Zhang, Y.M., 2009. First-principles study of half-metallic ferromagnetism in Zn1−xCrxSe. *Journal of magnetism and magnetic materials*, *321*(3), pp.198-202.

Szotek, Z., Temmerman, W.M., Svane, A., Petit, L., Stocks, G.M. and Winter, H., 2004. Half-metallic transition metal oxides. *Journal of magnetism and magnetic materials*, *272*, pp.1816-1817.

Song, W., Wang, J. and Wu, Z., 2009. Half metallic properties of Sr2CuOsO6. *Chemical Physics Letters*, *482*(4-6), pp.246-248.

Zhang, Y., Liu, W. and Niu, H., 2008. Half-metallic ferromagnetism in Cr-doped AlP—density functional calculations. *Solid state communications*, *145*(11-12), pp.590-593.

Saeed, Y., Nazir, S., Shaukat, A. and Reshak, A.H., 2010. Ab-initio calculations of Co-based diluted magnetic semiconductors Cd1− xCoxX (X= S, Se, Te). *Journal of magnetism and magnetic materials*, *322*(20), pp.3214-3222.

Lv, S., Li, H., Han, D., Wu, Z., Liu, X. and Meng, J., 2011. A better ferrimagnetic half-metal LuCu3Mn4O12: Predicted from first-principles investigation. *Journal of magnetism and magnetic materials*, *323*(5), pp.416-421.

Heusler, F., 1903. Über magnetische manganlegierungen. *Verhandlungen der Deutschen Physikalischen Gesellschaft*, *5*, p.219.

Luo, H., Zhu, Z., Ma, L., Xu, S., Liu, H., Qu, J., Li, Y. and Wu, G., 2007. Electronic structure and magnetic properties of Fe2YSi (Y= Cr, Mn, Fe, Co, Ni) Heusler alloys: a theoretical and experimental study. *Journal of Physics D: Applied Physics*, *40*(22), p.7121.

Hamad, B.A., 2011. The effect of defects on the electronic structure and magnetic map of the Fe 2 CrSi Heusler alloy: ab-initio calculations. *The European Physical Journal B*, *80*, pp.11-18.), p. 11

Ko, V., Qiu, J., Luo, P., Han, G.C. and Feng, Y.P., 2011. Half-metallic Fe2CrSi and non-magnetic Cu2CrAl Heusler alloys for current-perpendicular-to-plane giant magneto-resistance: First principle and experimental study. *Journal of applied physics*, *109*(7), p.07B103.

IEER Institute for Excellence in Education & Research